Gyrokinetic simulation of the Edge radial electric field generated by the ion orbit loss in tokamak

Shiqi Xiao[1], Yicheng Cai[1], Zihao Wang[1], and Shaojie Wang[1]

[1]*Department of Engineering and Applied Physics, University of Science and Technology of China, Hefei, 230023, China*

Introduction

The edge radial electric field (EREF) plays an important role in the L-H transition, and the ion orbit loss is thought crucial in the generation of the EREF in the tokamak plasma [1,2]. The gyrokinetic (GK) simulation is useful for investigating the ion orbit loss effect, and thus the PIC code XGC [2] and the Eulerian code COGENT [3] are developed for this purpose. In the past decade, the nonlinear GK global code NLT [4] based on the Numerical Lie-Transform method, which avoids the noise brought by the PIC code and reduces the Courant-Friedrichs-Lewy (CFL) restriction in the Eulerian code, has been developed and used to investigate the core plasma [4]. Motivated by the unique advantages and the success in the core plasma simulation, we extend the function of the NLT code to simulate the edge plasma with limiter configuration. We also perform some benchmark tests, and the simulation results agree with the analytical results [1,5]. In our simulation, the EREF is generated by the ion orbit loss of the initial Maxwellian distribution. The system reaches the quasi-steady state after several transit time periods of the thermal ion. The width of the quasi-steady state EREF pedestal is about a half banana width of the thermal ion, and the magnitude of the quasi-steady state electrostatic potential pedestal is roughly proportional to the edge ion temperature.

Brief review of the NLT code

The evolution of the ion gyrocenter distribution function $f(\boldsymbol{Z},t)$ is described by the gyrokinetic Vlasov equation (GKVE)

$$\partial_t f + \{f, H_0 + H_1\} = 0, \tag{1}$$

with $\{\cdots,\cdots\}$ denoting the Poisson bracket and $\boldsymbol{Z} = (\boldsymbol{X}, v_\parallel, \mu)$, where $\boldsymbol{X}$, $v_\parallel$, μ represent the gyrocenter position, parallel velocity and magnetic moment, respectively. $H_0 = \frac{1}{2}mv_\parallel^2 + \mu B$ and $H_1 = e_i\hat{J}_0\delta\varphi$ are the equilibrium and perturbed Hamiltonian, respectively, with $e_i, B, \hat{J}_0$ the ion charge, the equilibrium magnetic field and the gyro-average operator, respectively. The perturbed electrostatic potential $\delta\varphi$ is solved by the quasi-neutrality equation with the adiabatic electron

$$\frac{e_\mathrm{i}^2}{T_{0\mathrm{i}}}\int d^3v f_0\left(\delta\varphi - \hat{J}_0^2\delta\varphi\right) = e_\mathrm{i}\int d^3v\delta f + e_\mathrm{e}^2 n_{0\mathrm{e}}\frac{\delta\varphi - \langle\delta\varphi\rangle}{T_{0\mathrm{e}}}, \tag{2}$$

with $e_\mathrm{e}, T_{0\mathrm{i}}, T_{0\mathrm{e}}, n_{0\mathrm{e}}$ the electron charge, ion and electron equilibrium temperature, electron equilibrium density, respectively, and $\langle\cdots\rangle$ denoting the flux-surface average operator. The boundary condition is $\delta\varphi = 0$ at and out of the last closed flux surface (LCFS). The ion gyrocenter distribution function is divided into two parts $f(\boldsymbol{Z},t) = f_0(\boldsymbol{Z}) + \delta f(\boldsymbol{Z},t)$, where the equilibrium part satisfies $\{f_0, H_0\} = 0$. The NLT code solves the GKVE by using the Lie-transform

$$\bar{Z}^i = Z^i + G_1^i + \frac{1}{2} G_1^j \partial_j G_1^i, \quad 3$$

where the 1st order generating vector G_1^i is computed by $G_1^i = \{S_1, Z^i\}$ and the gauge function S_1 satisfies $\partial_t S_1 + \{S_1, H_0\} = H_1$. In the new coordinate, the GKVE is transformed to $\partial_t \bar{f} + \{\bar{f}, H_0\} = 0$, with the scalar invariance $\bar{f}(\bar{\boldsymbol{Z}}, t) = f(\boldsymbol{Z}, t)$. The steps of solving the GKVE in the NLT code for a given time interval $[t^n, t^{n+1}]$ are as follows:

(1) Set $S_1(\boldsymbol{Z}, t^n) = 0$.

(2) Solve $\partial_t \bar{f} + \{\bar{f}, H_0\} = 0$ by using the characteristic line method $\bar{f}(\bar{\boldsymbol{Z}}, t^{n+1}) = \bar{f}(\bar{\mathcal{Z}}(t^n; \bar{\boldsymbol{Z}}, t^{n+1}), t^n)$, where $\bar{\mathcal{Z}}(t^n; \bar{\boldsymbol{Z}}, t^{n+1})$ denotes the phase space point at t^n, which passes through $\bar{\boldsymbol{Z}}$ at t^{n+1} along the unperturbed orbit. If $\exists \tau \in [t^n, t^{n+1}] \Rightarrow \bar{\mathcal{Z}}(\tau; \bar{\boldsymbol{Z}}, t^{n+1}) \in L$, with L the limiter region, set $\bar{f}(\bar{\boldsymbol{Z}}, t^{n+1}) = 0$.

(3) Solve $\partial_t S_1 + \{S_1, H_0\} = H_1$ in the same way as step (2) $S_1(\bar{\boldsymbol{Z}}, t^{n+1}) = \int_{t^n}^{t^{n+1}} H_1(\bar{\mathcal{Z}}(\tau; \bar{\boldsymbol{Z}}, t^{n+1}), \tau) d\tau$.

(4) Pull back by using the scalar invariance $f(\boldsymbol{Z}, t^{n+1}) = \bar{f}(\bar{\boldsymbol{Z}}, t^{n+1})$.

Numerical tests

In this work, the equilibrium of a circular tokamak [5] is used, with the parameters listed in table 1, and the setup of the cases tested is listed in table 2. In the five cases tested, the density profile is uniform $n_{0e} = n_{0i} = n_{ref}$ and $T_{0i} = T_{0e}$ is used, with the reference density $n_{ref} = 10^{20}\mathrm{m}^{-3}$ and the reference temperature $T_{ref} = 1\mathrm{KeV}$. The fixed electrostatic potential in case 3 is $\frac{e_i \delta\varphi}{T_{ref}} = -1$ when $\frac{r}{a} \leq 0.8$, $\frac{e_i \delta\varphi}{T_{ref}} = -1 + \left(\frac{r/a - 0.8}{0.2}\right)^2$ when $\frac{r}{a} > 0.8$, and $\epsilon = \frac{r}{R_0}$ in table 1.

Parameter	Value	Parameter	Value
Major radius	$R_0 = 1.7\mathrm{m}$	Minor radius	$a = 0.6\mathrm{m}$
Magnetic field at the magnetic axis	$B_0 = 1.6\mathrm{T}$	Poloidal magnetic flux	$\psi = \frac{\mu_0 I_p R_0 r^2}{4\pi a^2}$
Safety factor	$q(r) = \frac{r^2 B_0}{2\psi\sqrt{1-\epsilon^2}}$	Total plasma current	$I_p = 1.3\mathrm{MA}$
Ion species	D^+	Initial distribution	Maxwellian f_M

Table 1: The equilibrium parameters.

Case	Initial T_{0i}/T_{ref}	Electrostatic potential	Purpose
1	$3.3 - 3r/a$	No	Benchmark
2	$3.8 - 3r/a$	No	Benchmark
3	$3.8 - 3r/a$	Fixed	Benchmark
4	$3.3 - 3r/a$	Self-consistent	EREF test
5	$3.8 - 3r/a$	Self-consistent	EREF test

Table 2: The setup of the cases tested.

A set of benchmark tests (case 1 to 3) of the collisionless relaxation have been carried out

between the NLT code and the analytical results [1,5]. The system reaches the quasi-steady state at about $100R_0/c_s$, with $c_s = \sqrt{T_{\mathrm{ref}}/m}$, which is several transit time periods of the thermal ion. Figure 1 shows that the quasi-steady state flux-surface averaged particle loss fraction $\langle P\rangle = \int f d^3v \,/\, \int f_M d^3v$ increases with the minor radius and the ion temperature. The quasi-steady state flux-surface averaged momentum loss fraction $\langle M\rangle = \int v_{\|} f d^3v \,/\, \int v f_M d^3v$ and the flux-surface averaged parallel rotation of the bulk ions $\langle v_{\|}\rangle = -\sqrt{8T_{0\mathrm{i}}/(\pi m)}\langle M\rangle$ increase to a peak and then decrease to zero at LCFS, and the peak moves inward for the higher ion temperature. Figure 2 shows that the loss cone appears at about $20R_0/c_s$, and the ions in the loss cone get loss almost totally at $100R_0/c_s$, when the system reaches the quasi-steady state. The loss cone is shifted to the high-energy tail in the presence of the radial electrostatic potential. These results agree with the analytical results [1,5].

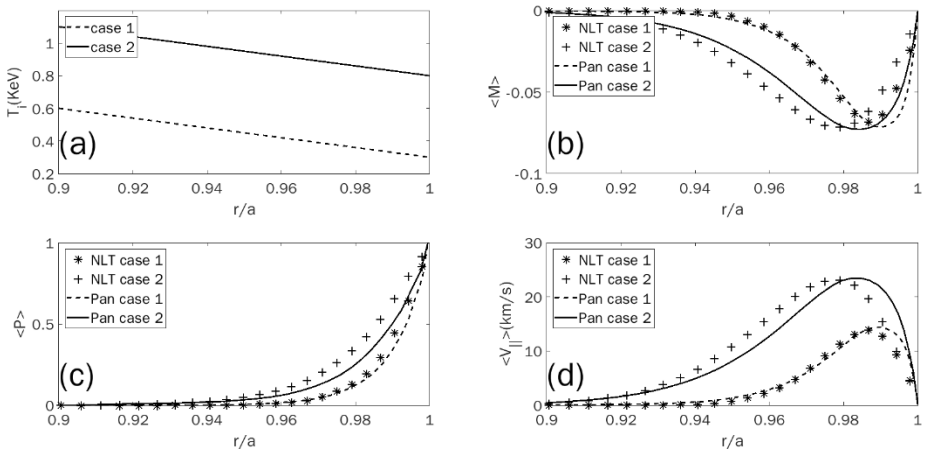

Figure 1: Profiles of (a) the ion temperature, (b) the flux-surface averaged momentum loss fraction, (c) the flux-surface averaged particle loss fraction, (d) the flux-surface averaged parallel rotation of the bulk ions, at $100R_0/c_s$, with the analytical results given by [5].

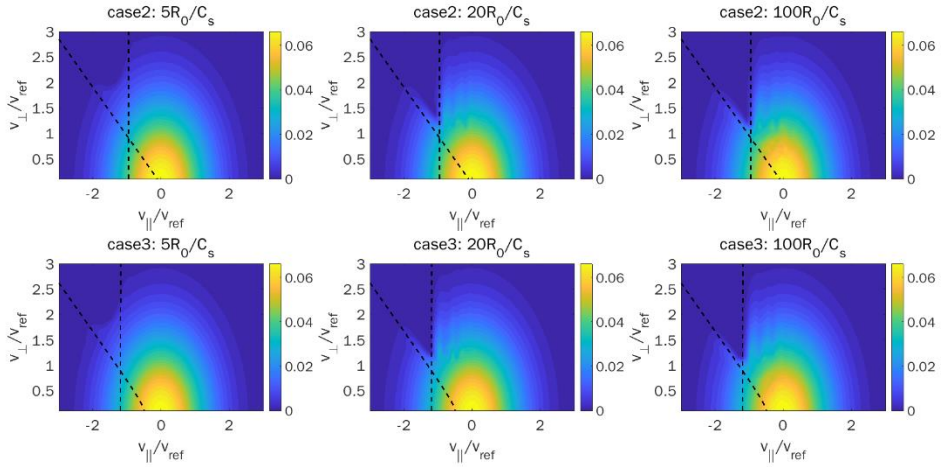

Figure 2: The evolution of f in the velocity space at $(r,\theta) = (0.95a, 0)$ for case 2 and 3, with the dashed curves representing the analytical results of loss cone given by [1].

The generation of the EREF (case 4 and 5) is investigated after the benchmark. Figure 3 shows that the quasi-steady state EREF generated by the ion orbit loss reaches the quasi-steady state at

about $100R_0/c_s$. Figure 3 also shows that the EREF reduces $\langle P \rangle$, which means the EREF suppresses the ion orbit loss in return. At the quasi-steady state, the electrostatic potential pedestal width and the width of $\langle P \rangle$ are both about a half banana width of the thermal ion, and the magnitude of the pedestal (in V) is about twice the ion temperature (in eV) at the top of the pedestal.

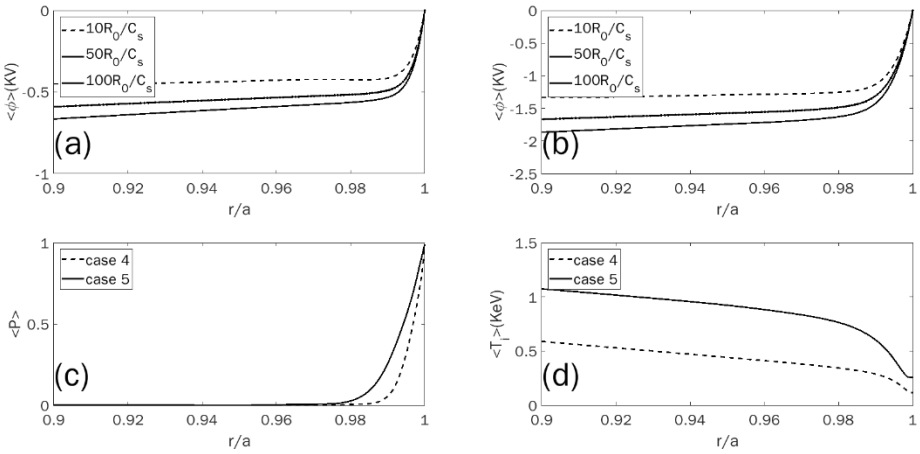

Figure 3: Profiles of (a) the flux-surface averaged electrostatic potential for case 4, (b) the flux-surface averaged electrostatic potential for case 5, (c) the flux-surface averaged particle loss fraction at $100R_0/c_s$, (d) the flux-surface averaged ion temperature at $100R_0/c_s$.

Conclusion

The function of the NLT code has been extended to simulate the edge plasma and the implementation has been benchmarked. By using the NLT code, we investigate the generation of the EREF, and obtain the semi-quantitative relationship between the plasma parameters and the electrostatic potential pedestal width and magnitude, which is important for the further research.

References

[1] X. Xiao, L. Liu, X. Zhang, and S. Wang, Phys. Plasmas 18, 032504 (2011)

[2] H. Zhu, T. Stoltzfus-Dueck, R. Hager, S. Ku, and C. S. Chang, Nucl. Fusion 62, 066012 (2022)

[3] M. A. Dorf, M. R. Dorr, J. A. Hittinger, R. H. Cohen, and T. D. Rognlien, Phys. Plasmas 23, 056102 (2016)

[4] Y. Xu, and S. Wang, Rev. Mod. Plasma Phys. 10, 2 (2026)

[5] C. Pan, S. Wang, and J. Ou, Nucl. Fusion 54, 103003 (2014)